Proceeding of the IEEE
International Conference on Robotics and Biomimetics
Dali, China, December 2019

Mechanism Design and ADAMS-MATLAB-Simulation of a Novel Ankle Rehabilitation Robot *

Zhengdi Sun, Chunbao Wang, Jianjun Wei, Quanquan Liu, Tong Wang, Zhixian Mao, Xiaojiao Chen, Lihong Duan, Xin Zhang, Guangshuai Zhang, Yulong Wang, Jianjun Long, Jianyi Li.

***Abstract*— As the population continues to grow, stroke has become one of the major diseases that threaten the health of the elderly people. As a product of combination of medicine and Engineering, the ankle rehabilitation robot can assist ankle joints patients with rehabilitation training and has a good prospect of application. This paper presents an ankle rehabilitation robot for hemiplegic patients. Firstly, the physiological structure of human ankle joint is introduced and the design requirements of robot are put forward. Then the three components of the robot mechanism (the internal/external rotation mechanism, the dorsiflexion/plantarflexion mechanism, the inversion/eversion mechanism) are described in detail and the motion range of each joint is analyzed. The dynamics model in ADAMS and the control model in Simulink of the novel ankle rehabilitation robot are built based on the mechanism model. Based on the ADAMS and MATLAB co-simulation technology, dynamics analysis and control analysis of the ankle rehabilitation robot are carried out. Compared with experimental data, the simulation results show the feasibility of the mechanism design and control scheme. The difficulties and practicability of the co-simulation technology in the ankle rehabilitation robot are further discussed.**

I. Introduction

Stroke is a disease with a high incidence rate and high disability rate among the elderly. Among them, 80-90% of stroke survivors often have sequelae of hemiplegia [1-2]. As a distal joint, the ankle joint plays an important role in the rehabilitation of the nervous system. And the ankle joint rehabilitation training is the prerequisite for patients with hemiplegia to recover their walking ability. The traditional rehabilitation method is to manually assist the patient to complete the training movement of the ankle joint by the physical therapist [3]. The traditional training method is single, and it also puts a heavy burden on the physiotherapist which limits the rehabilitation efficiency.

With the advancement of technology, rehabilitation robots have attracted the attention of researchers at home and abroad as an emerging treatment method. Ankle rehabilitation robot can be divided into three types: traditional robot, parallel robot and exoskeleton robot according to mechanical structure. Traditional robots such as VRACK from Northeastern University [4-5], Ankle rehabilitation robot from Tsinghua University [6], its function is relatively simple. Parallel robot such as Rutgers from Rutgers University [7], Ankle rehabilitation robot from Hebei University of Technology [8], its control is complicated. Exoskeleton robot such as PAFO from National Institutes of Health [9-10], wearable ankle rehabilitation robot from Nanyang Technological University [11], medical exoskeleton system from Zhejiang University [12], it has the disadvantages of complicated mechanism and inconvenient wear, and it is not suitable for early clinical patients. Therefore, this article presents a new ankle rehabilitation robot with serial structure to improve the rehabilitation effect of patients.

II. Mechanism Design

A. Demand analysis

According to the theories of Continuous Passive Motion (CPM) and Continuous Active Motion (CAM) [13], hemiplegia patients can reshape the central nervous system and restore the joint mobility through appropriate rehabilitation training.

* Research supported by National Natural Science Foundation of China (No.61703282, No.61963007), National Natural Science Foundation of China and Shenzhen Robot Research Program (No.U1613221), Research Foundation of Beijing Advanced Innovation Center for Intelligent Robots and Systems (No.2018IRS08, No.2018IRS07), Natural Science Foundation of Guangdong Province (No. 2018A030313028), Technology Research Foundation of Basic Research Project of Shenzhen (No.JCYJ20170413095245139, No. JCYJ20170306170851910), Research Foundation of Health and Family Planning Commission of Shenzhen Municipality (Grants No. SZBC2017006),Shenzhen Dapeng New District Medical Health Group Research Project (No. 2019JTYM001).

Zhengdi Sun is with the Guangxi University of Science and Technology, Liuzhou, CO 54500 China (e-mail: ZhengdiSUN@163.com).

Chunbao Wang is with the Shengzhen Institute of Geriatrics and Guangxi University of Science and Technology, The First Affiliated Hospital of Shenzhen University, Shenzhen, CO 518035 China, (corresponding author to provide phone: 0755-3281-6725; e-mail: chunbaowang@szu.edu.cn).

Jianjun Wei is with the Guangxi University of Science and Technology, CO 54500 China (e-mail: weijianjun629@163.com).

Quanquan Liu is with the Shengzhen Institute of Geriatrics, The First Affiliated Hospital of Shenzhen University,CO 518035 China, (e-mail: wphdliu@163.com).

Tong Wang is with the Guangxi University of Science and Technology, CO 54500 China (e-mail: wt602949579@163.com).

Xiaojiao Chen is with the MK Smart Robotics Co., Ltd, CO 518110 China, (e-mail: xjchen@mkrobotics.cn).

Zhixian Mao is with the Guangxi University of Science and Technology, Liuzhou, CO 54500 China (e-mail: 1943256385@qq.com).

Lihong Duan is with the Shengzhen Institute of Geriatrics, The First Affiliated Hospital of Shenzhen University,CO 518035 China, (e-mail: missduan2004@163.com).

Xin Zheng is with Shenzhen Dapeng New District Nan'ao People's Hospital, CO 518116, China, (e-mail: wphdliu@163.com).

Guangshuai Zhang is with the Guangxi University of Science and Technology, Liuzhou, CO 54500 China (e-mail: 1203604933@qq.com).

Yulong Wang is with the First Affiliated Hospital of Shenzhen University, (e-mail: ylwang66@126.com).

Jianjun Long is with the First Affiliated Hospital of Shenzhen University, (e-mail: 345399075@qq.com).

Jianyi Li is with the Southern Medical University, (e-mail: wuxili74@126.com).

978-1-7281-6321-5/19//$31.00 ©2019 IEEE

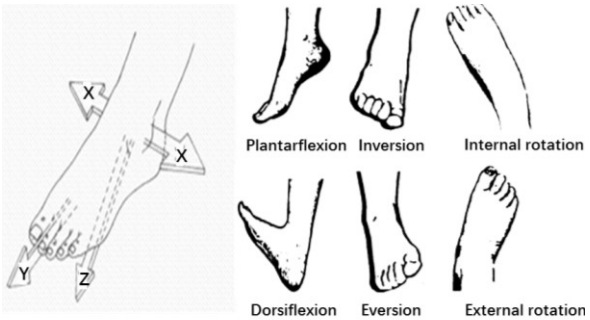

Figure 1 The movements of the human ankle joint

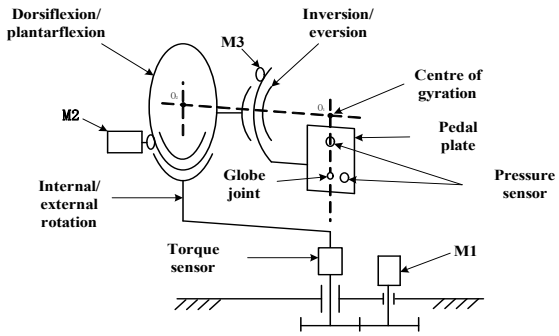

Figure 2 The schematic diagram of the rehabilitation robot

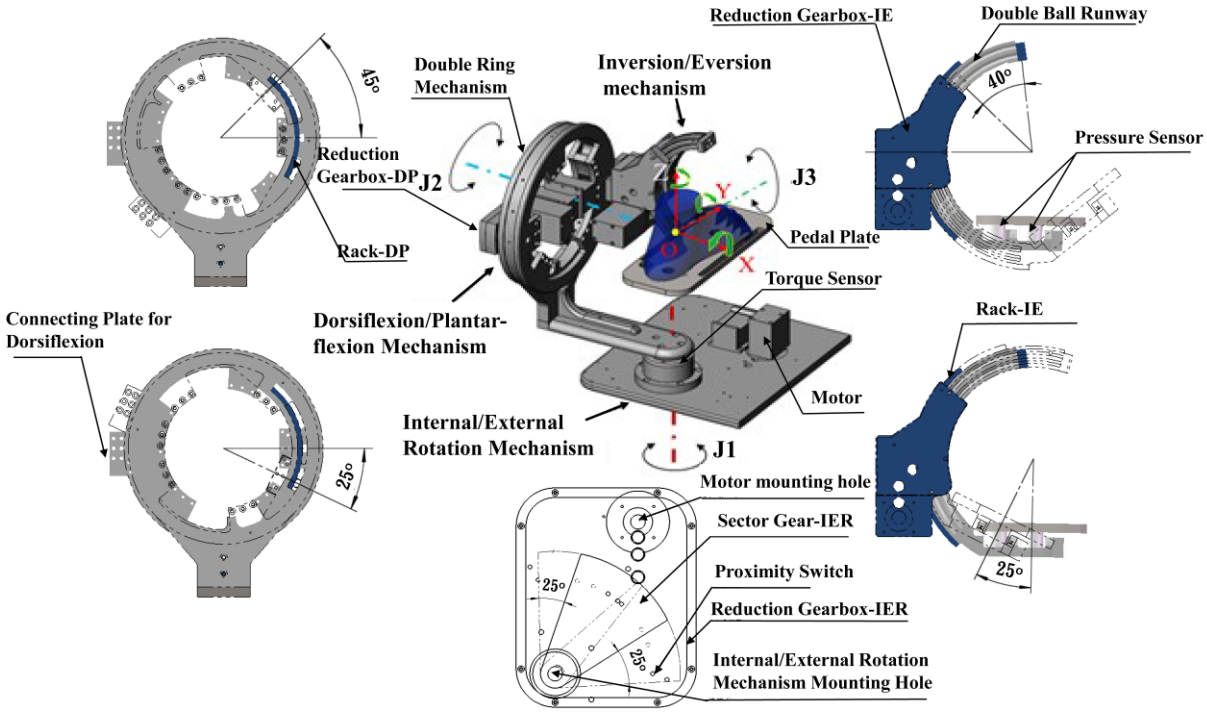

Figure 3 The whole mechanism of the novel rehabilitation robot

The coordinate system of ankle joint is established with the coronal axis as the X-axis, the vertical axis as the Y-axis, and the sagittal axis as the z-axis. And the physiological motion of the ankle joint can be divided into six actions include the movements of dorsiflexion and plantarflexion around the X-axis, the movements of internal rotation and the external rotation around the Y-axis, and the movements of inversion and eversion around the Z-axis (see Fig. 1). In addition, the three rotational movements of the ankle joint can be performed separately or simultaneously, and the movement parameters of the human ankle joint are as shown in the TABLE Ⅰ.

TABLE I. THE PARAMETERS OF ANKLE MOVEMENTS

Motion	Parameter		
	Angle range (°)	*Angular velocity range (°/s)*	*Angular acceleration range (°/s²)*
Internal	0~20	40	60
External	0~30		
Dorsiflexion	0~30	60	78
Plantarflexion	0~50		
Inversion	0~40	100	90
Eversion	0~30		

B. *Structure Design*

The novel ankle joint rehabilitation robot adopts bilateral symmetrical mechanism design to meet the rehabilitation training mode of the affected side follows the movement of the intact side. The single mechanism can be divided into three parts include the internal/external rotation mechanism, the dorsiflexion/plantarflexion mechanism, and the inversion/eversion mechanism to meet the requirements of three degrees of freedom of rotation movement of the ankle joint. Each motion mechanism uses the DC brushless motor for servo drive, and the transmission system is mainly composed of the reduction gearbox and the gear. The

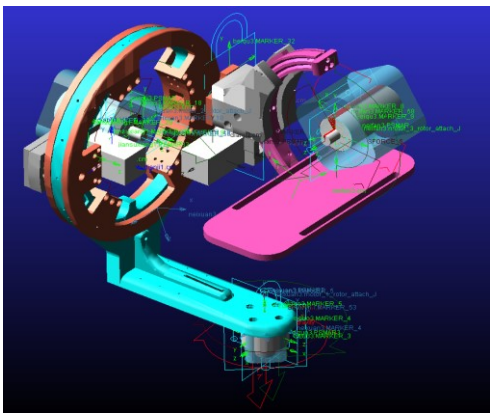

Figure 4 The ADAMS model of the robot

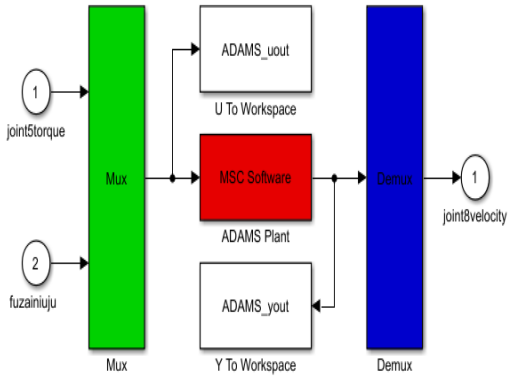

Figure 5 The co-simulation model of ADAMS and MATLAB

scheme of the single ankle rehabilitation robot is shown in figure.

The base is an important part of the ankle rehabilitation robot which plays a role of fixing and supporting other parts of the robot. The bottom plate is made of aluminum plate with size of 600mm×350mm×15mm, and the mounting holes above are designed with bilateral symmetry. The internal/external rotation mechanism is connected to the base through the rotary pair, the drive motor and the proximity switch are mounted on the upper surface of the bottom plate, and the reduction gearbox-IER is mounted on the lower surface of the bottom plate.

The internal/external rotation mechanism is designed as an L-shaped connecting rod, and one end of the connecting rod is connected by a torque sensor and the rotating sector gear. The other end of the connecting rod is connected to the dorsiflexion/plantarflexion mechanism through a circular mechanism. The torque sensor is mounted inside the rotating pair of the internal/external rotation mechanism to measure the force of the patient's ankle joint and realize the torque control of the robot. The rotation axis of the internal/external rotation is perpendicular to the surface of the bottom plate, and the L-shaped connecting rod and the torque sensor are connected to the bottom plate through the rotating pair. A rack is mounted on the circular mechanism to achieve the movement of the dorsiflexion/plantarflexion mechanism. At the same time, the circular grooves are designed on both sides of the circular mechanism, and the balls are in contact with the dorsiflexion/plantarflexion mechanism. The sector gear-IER is arranged on the lower surface of the bottom plate and is driven by the reduction gearbox-IER and the gear shaft of the motor.

The dorsiflexion/plantarflexion mechanism is mounted on the external rotation mechanism and connected with the inversion/eversion mechanism. The dorsiflexion/plantarflexion mechanism is designed as a complete double ring structure to maintain its stiffness and stability. The reduction gearbox-DP is fixed to the connecting frame of the inversion/eversion mechanism. The connecting frame is provided with a mounting hole for motor, which makes the ankle rehabilitation robot compact in structure. The dorsiflexion/plantarflexion mechanism and the internal/external rotation mechanism are slid with the circular groove and the ball during the rotation, so that the rotational axis of the dorsiflexion/plantarflexion mechanism is fixed. This design idea makes the whole mechanism equivalent to a large bearing, and the mechanism moves smoothly, the frictional resistance during movement is greatly reduced.

The inversion/eversion mechanism is located at the end of the ankle rehabilitation robot which is in contact with the human body through the foot pedal. The whole inversion/eversion mechanism is designed as a C-shaped link to reduce the weight of the robot and facilitate the rehabilitation training. The rack-IE is installed in the C-shaped link, which can transmit the power from the motor through the reduction gearbox-IE. The inversion/eversion mechanism is connected to the dorsiflexion/plantarflexion mechanism through the reduction gearbox-IE, and the double-ball-spout design is adopted to increase the stability of the inversion/eversion mechanism. Two pressure sensors are arranged under the foot pedal to measure the force of the dorsiflexion/plantarflexion movement and inversion/eversion movement of the ankle joint of the human body, and it can be achieved the torque control.

The ankle joint rehabilitation robot is used for rehabilitation training of ankle joint patients. In order to prevent secondary injury to the patient, the range of motion of the ankle joint rehabilitation robot is limited through the limit mechanism and the proximity switch based on the ankle joint motion parameters. The motion range of the three motion units is as shown in TABLE Ⅱ. By comparing the actual range of motion of the robot with the motion range of the human ankle joint, the mechanism design of the new ankle joint rehabilitation robot meets the physiological needs of the human ankle joint

TABLE II. THE MOVEMENT RANGE OF THE ROBOT

Mechanism	**Parameter**	
	Motion	***Angle range (°)***
Internal/external rotation mechanism	Internal	0~20
	External	0~30
Dorsiflexion/plantarflexion mechanism	Dorsiflexion	0~30
	Plantarflexion	0~50
Inversion/ eversion mechanism	Inversion	0~40
	Eversion	0~30

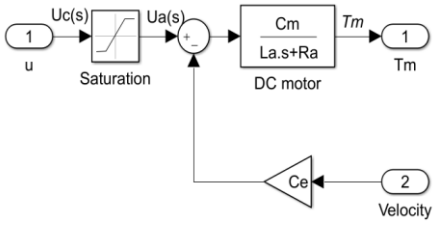

Figure 6 The modle of the motor in Simulink

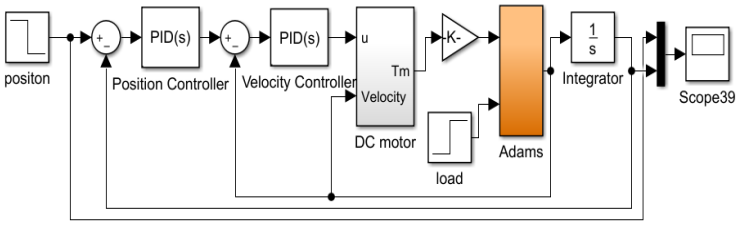

Figure 8 The framework of speed control

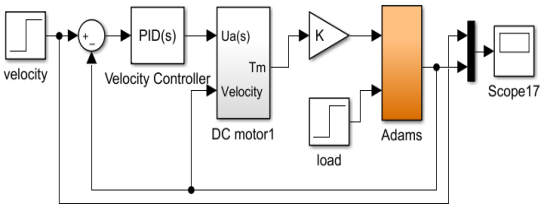

Figure 7 The framework of position control

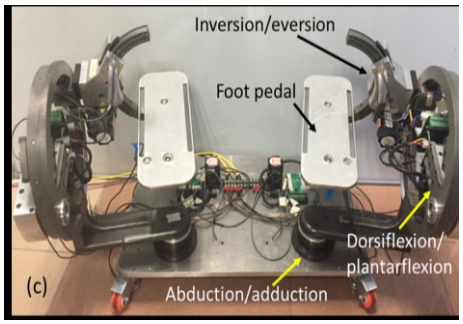

Figure 9 The prototype of the ankle joint rehabilition robot

III. ADAMS AND MATLAB CO-SIMULATION

A. *ADAMS Dynamics Model*

The model of the ankle rehabilitation robot was simplified and imported into ADAMS software. The initial coordinate value and the corresponding material to each mechanism of the robot are set in ADAMS (the main material is 45 steel and 5052 aluminum). After setting the constraint and motion mode of the parts is finished, the dynamics model of this robot in ADAMS is established.

According to the analysis of mechanism dynamics [14], the movement of three joints are same during the training of the robot. However, the force on the dorsiflexion/plantarflexion mechanism is relatively complex, so the dorsiflexion/plantarflexion mechanism is selected as the object of the co-simulation. The internal and external rotation mechanism is located below the dorsiflexion/plantarflexion mechanism and does not affect the movement of the dorsiflexion mechanism. The inversion/eversion mechanism and the dorsiflexion/plantarflexion mechanism remain relatively stationary. In order to simulate the actual situation better, the brushless dc servo motor and the pinion reduction box are added, the dynamic model of single movement of dorsiflexion/plantarflexion mechanism is established as shown in the Fig. 4.

The data variables that need to be exchanged for co-simulation include: the drive torque of the pinion (the output of the drive motor), the load of the pedal (load end), and the angular velocity of the dorsiflexion mechanism (load end). The first two variables are used as the input variables of the ADMAS control model, and the last variable is used as the output variable of the ADMAS control model. The ADAMS and MATLAB co-simulation model is exported through the Controls module of ADAMS, as shown in Fig. 5

B. *Brushless DC Motor Control Model*

The control model of brushless DC motors is dual closed-loop control of current and speed, and the modelling process is complicated. In order to reduce the computational complexity of the co-simulation, the PWM speed regulation mode of the brushless DC motor is converted to the voltage speed regulation mode of the ordinary DC motor. The model of the DC motor servo system can be divided into two parts: the electric circuit model of the motor and the force balance model of the transmission mechanism. The transfer function is as shown below:

$$\dot{\theta}_m(s) = \frac{C_m}{J_m s + B_m} I_a(s) - \frac{T_L}{J_m s + B_m} \quad (1)$$

According to formula (3), the open loop control model of the electric circuit of the DC motor is established in the Simulink module of MATLAB, as shown in Fig. 6. The actual working range of the DC motor is limited , considering the saturation characteristic of the input voltage of the driver, a voltage limiting module (-24V~24V) is added. The force balance model of the transmission is replaced by the ADAMS dynamics model.

C. *PID Control System*

The brushless DC motor can detect the rotor speed of the motor through the incremental photoelectric encoder at the end of the motor, and the encoder feeds back the signal to the controller. The controller further calculates the deviation between the desired speed and the feedback speed to obtain the control amount. The controller transmits the control amount to the driver, and finally the driver drives the DC motor to rotate. The PID regulator is simple and the parameters are easy to set. Therefore, the PID algorithm is generally used to control the speed of the motor. The control framework is shown in Fig. 7.

The differential action in the PID control algorithm is too sensitive, which will cause the system control process to oscillate and reduce the adjustment quality. Therefore, the incomplete differential controller is used in this system. The standard form of the incomplete differential controller is as shown below:

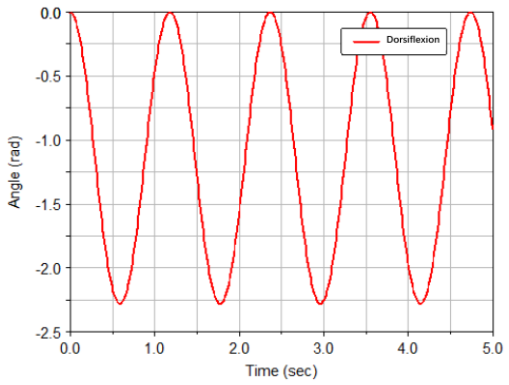

Figure 10 The movement curve of the dorsiflexion mechanism under the action of gravity

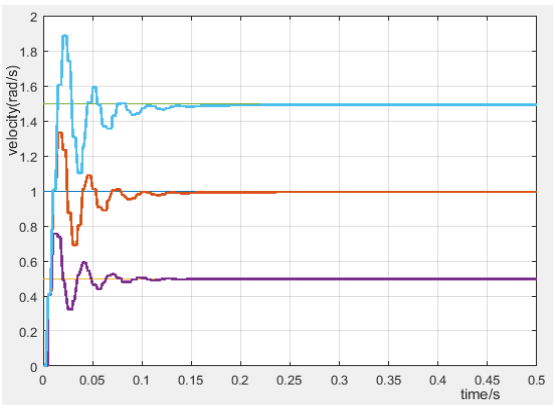

Figure 11 The curve of speed response experiment

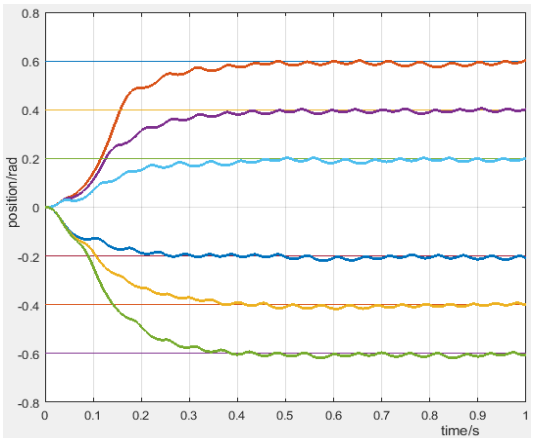

Figure 12 The curve of position control experiment

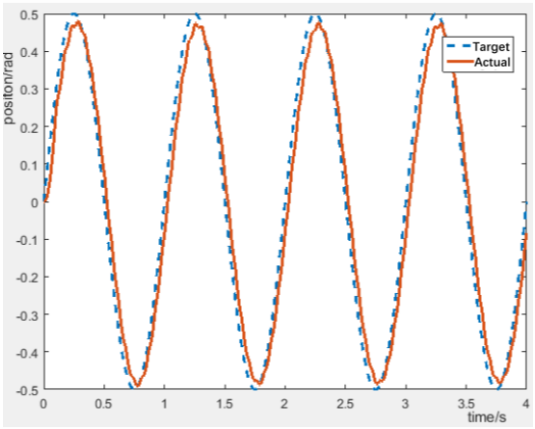

Figure 13 The curve of position accuracy experiment

$$C(s) = P + D\frac{N}{1+\frac{1}{s}N} \quad (2)$$

Based on the closed-loop speed control, the PID control is performed on the position loop of the motor. The control framework is shown in Fig. 8. In order to prevent secondary injury to the patient, the ankle rehabilitation robot does not require a high response speed and requires high positioning accuracy. Therefore, the system needs to be designed as a position-free-overshoot system, and this can be achieved by using PD control.

IV. EXPERIMENT

A. Experiment Platform

According to the design scheme of the whole mechanism, the prototype of the new ankle joint rehabilitation robot was developed as shown in Fig.9. Among them, the model of the brushless DC motor used in dorsiflexion mechanism is ECFlat45 from Maxon, and its power is 70W. The rated voltage of the motor is 24V, the rated speed is 3000 rpm, and the rated torque is 0.369N.m. When the transmission ratio of the dorsiflexion mechanism is 172, the rated rotational speed of the dorsiflexion flexion mechanism can reach 17.4 rpm, and the rated torque can reach 63.3 N.m, which satisfies the movement requirement of the dorsiflexion mechanism. Motor driver is selected as IBL3605A intelligent servo driver, which is based on DSP and set motion control, drive and PLC functions in one unit.

Open the parameter setting software of the driver and measure the motor parameters as follows: Torque constant Cm=0.0369 Nm/A, Phase resistance Ra=0.608 Ω , Phase inductance La=0.463mH, The control model of motor can be set by the above parameters.

B. Simulation Under Gravity

In the initial state, the various mechanisms of the new ankle rehabilitation robot are in the middle position. This section simulates the motion of the mechanism with gravity only that mean the drive function of the mechanism is equal to zero. The dorsiflexion mechanism reciprocates under the action of gravity, and its motion curve is shown in Fig. 10.

The Fig. 10 shows that the initial center of the dorsiflexion mechanism is not on the axis of rotation, the gravity of the dorsiflexion mechanism is not balanced during the movement. The potential energy and kinetic energy of the dorsiflexion/plantarflexion mechanism are converted by reciprocating motion, which will affect the motion control of the dorsiflexion mechanism.

C. Speed Response

The speed response experiment of the motor is carried out with the speed of 0.5rad/s, 1rad/s and 1.5rad/s, and the simulation time is 1s. The optimal PID parameters of the speed controller are: P=13.15, D=0.548, N=100, the simulation results are shown in Fig. 11.

The simulation results of speed response show that the dorsiflexion/plantarflexion mechanism reached the specified speed in 0.02s and keep this speed constant. Although there is always a slight deviation between the actual speed and the theoretical speed, the mechanism responds to instructions quickly and meets the design requirements.

D. Position Control Experiment

The PID position control experiment of the motor is carried out with the speed of ±0.6rad，±0.4rad，±0.2rad, and the simulation time is 1s. With the PID parameters of the speed controller unchanged, the optimal PID parameters of the position controller are obtained after tuning: P=34, D=1.3, N=100, the simulation results are shown in Fig. 12.

The simulation results of PID position control show that the dorsiflexion/plantarflexion mechanism reaches the designated position after 0.4s, but the mechanism is unstable and always in the process of oscillation. Under the same control parameters, the position control amount of dorsiflexion has no overshoot, and the position of the flexion movement is overshoot. This is due to the influence of gravity, which indicating that the PID position control accuracy of the dorsiflexion/plantarflexion mechanism is affected by the position of the mechanism.

E. Position Accuracy Experiment

In the rehabilitation training of ankle joint patients, the dorsiflexion/plantarflexion mechanism is not always at a certain speed or a certain position, but moves back and forth in accordance with a certain frequency. Therefore, the experiment of position precision can reflect the motion characteristics of ankle rehabilitation robot. The input of the position control simulation changed from step signal to sinusoidal signal with the amplitude of 0.5rad and the frequency of 1Hz. Keep the PID parameters of the speed controller and the position controller, and the simulation results are shown in Fig. 13. In the figure, the dotted line represents the expected trajectory, and the solid line represents the actual trajectory.

The simulation results of the motion trajectory control show that the actual motion trajectory of the dorsiflexion mechanism can follow the expected motion trajectory. Although there is a slight delay in the movement of the actual trajectory and vibration occurs at the limit position of dorsiflexion movement, the velocity response is faster and the position accuracy is higher.

V. CONCLUSION

This paper introduces a novel ankle rehabilitation robot for stroke patients. Based on the analysis of the complete mechanism of the novel ankle rehabilitation robot, the control performance of the dorsiflexion/plantarflexion mechanism of the robot was analyzed through ADAMS and MATLAB co-simulation technology.

Same factors such as gear transmission friction and gear transmission gap were not considered in the simulation process, which causes the simulation to run differently from the actual situation. However, the simulation results are consistent with the experimental data of the prototype, which indicating that the co-simulation achieves the expected purpose. Experiments show that the novel ankle joint rehabilitation robot has a reasonable design of the dorsiflexion mechanism, with good response characteristics and high positional accuracy, which meeting the design requirements.

The motion control of ankle rehabilitation robot is a complex nonlinear system. In order to make the new ankle rehabilitation robot run more stable, it is necessary to adjust the mechanism design scheme, choose the motor with better performance or adopt other advanced control schemes. In the future work, the control system of the robot will be further improved and the dynamic performance of the robot and the control characteristics of the whole mechanism will be analyzed. Furthermore, the clinical experiment will be carried out to verify the robot's function of rehabilitation.

REFERENCES

[1] B. Li, G. Li, Y. Sun, et al., “A Review of Rehabilitation Robot”, *in Proc. 32nd Youth Academic Annual Conference of Chinese Association of Automation (YAC)*, Hefei, 2017, pp. 900–901.

[2] C. Grigore, P. Kevin, “A Review of Integrative Virtual Games for Rehabilitation”, *in Proc. 2017 E-Health and Bioengineering Conference*, Sinaia, 2017, pp. 733–736.

[3] C B. Wang, Z D. Sun, J J. Wei, et al., “Systemic design of an NARR for hemiplegic survivors”, *The Journal of Engineering*, vol. 2019, no. 14, pp. 522-529, 2001.

[4] R. Ranky, M. Sivak, J. Lewis, et al., “VRACK — virtual reality augmented cycling kit: Design and validation”, *in Proc. 2010 IEEE Virtual Reality Conference (VR)*, Waltham ,2010 pp.135-138.

[5] A B. Farjadian, Q. Kong; V K. Gade, et al., “VRACK: Measuring pedal kinematics during stationary bike cycling”, *in Proc. 2013 IEEE 13th International Conference on Rehabilitation Robotics (ICORR)* Seattle, 2013, pp. 1-6.

[6] Z. Zhou, Y. Zhou, N. Wang, et al., “On the design of a robot-assisted rehabilitation system for ankle joint with contracture and/or spasticity based on proprioceptive neuromuscular facilitation”, *in Proc. 2014 IEEE International Conference on Robotics and Automation (ICRA)* Hong Kong, 2014, pp. 736-741.

[7] M. Girone, G. Burdea, M. Bouzit, et al., “A Stewart Platform-Based System for Ankle Telerehabilitation”, *Autonomous Robots*, vol. 10, no. 2, pp. 203-212, 2001.

[8] G. Liu, J. Gao, S. Yang, et al., “The Configuration of the Ankle Rehabilitation Exercises Parallel Mechanism and its Kinematics Analysis”, *Development & Innovation of machinery & electrical products*, vol. 18, no. 5, pp. 13-15, 2005.

[9] J. Ward, T. Sugar, J. Standeven, et al., “Stroke survivor gait adaptation and performance after training on a Powered Ankle Foot Orthosis”, *in Proc 2010 IEEE International Conference on Robotics and Automation, Anchorage*, 2010, pp. 211-216.

[10] A M. Oymagil, J K. Hitt, T. Sugar, et al. Control of a Regenerative Braking Powered Ankle Foot Orthosis, *in Proc 2007 IEEE 10th International Conference on Rehabilitation Robotics,* Noordwijk, 2007, pp. 28-34.

[11] S M M. Rahman, R. Ikeura, “A Novel Variable Impedance Compact Compliant Ankle Robot for Overground Gait Rehabilitation and Assistance” *Procedia Engineering*, vol.41, pp. 522-531, 2012.

[12] H. Yu, “Development of A Wearable Three-degree-of-freedom Ankle exercise rehabilitation exoskeleton system”, Zhejiang University, Hangzhou, ME, 2012.

[13] R B. Salter, P. Field, “The Effects of Continuous Compression on Living Articular Cartilage: An Experimental Investigation”, *Journal of Bone & Joint Surgery*, vol. 42, no.1, pp. 31-49,1960.

[14] Z D. Sun, C B. Wang; J J. Wei, et al., “Kinematics and Dynamics Analysis of a Novel Ankle Rehabilitation Robot”, *in Proc. 9th IEEE International Conferenceon CYBER Technology in Automation, Control, and Intelligent Systems,* Suzhou, 2019, pp. 1404-1409.